

Measurement of $B(D_s^+ \rightarrow \mu^+ \nu_\mu)$

L. Widhalm,¹⁰ I. Adachi,⁷ H. Aihara,⁴² T. Aushev,^{17,12} A. M. Bakich,³⁸ V. Balagura,¹² E. Barberio,²⁰ A. Bay,¹⁷ I. Bedny,¹ V. Bhardwaj,³² U. Bitenc,¹³ S. Blyth,²⁴ A. Bozek,²⁶ M. Bračko,^{19,13} J. Brodzicka,⁷ T. E. Browder,⁶ Y. Chao,²⁵ A. Chen,²³ W. T. Chen,²³ B. G. Cheon,⁵ R. Chistov,¹² I.-S. Cho,⁴⁷ Y. Choi,³⁷ J. Dalseno,²⁰ M. Dash,⁴⁶ A. Drutskoy,³ S. Eidelman,¹ P. Goldenzweig,³ B. Golob,^{18,13} H. Ha,¹⁵ J. Haba,⁷ K. Hayasaka,²¹ H. Hayashii,²² M. Hazumi,⁷ D. Heffernan,³¹ Y. Hoshi,⁴⁰ W.-S. Hou,²⁵ Y. B. Hsiung,²⁵ H. J. Hyun,¹⁶ T. Iijima,²¹ K. Inami,²¹ A. Ishikawa,³⁴ H. Ishino,⁴³ R. Itoh,⁷ M. Iwasaki,⁴² Y. Iwasaki,⁷ D. H. Kah,¹⁶ J. H. Kang,⁴⁷ P. Kapusta,²⁶ N. Katayama,⁷ H. Kawai,² T. Kawasaki,²⁸ H. Kichimi,⁷ S. K. Kim,³⁶ Y. J. Kim,⁴ K. Kinoshita,³ S. Korpar,^{19,13} P. Križan,^{18,13} P. Krokovny,⁷ R. Kumar,³² C. C. Kuo,²³ Y. Kuroki,³¹ A. Kuzmin,¹ Y.-J. Kwon,⁴⁷ J. Lee,³⁶ J. S. Lee,³⁷ M. J. Lee,³⁶ S. E. Lee,³⁶ T. Lesiak,²⁶ S.-W. Lin,²⁵ C. Liu,³⁵ D. Liventsev,¹² F. Mandl,¹⁰ A. Matyja,²⁶ S. McOnie,³⁸ W. Mitaroff,¹⁰ H. Miyake,³¹ H. Miyata,²⁸ Y. Miyazaki,²¹ R. Mizuk,¹² G. R. Moloney,²⁰ E. Nakano,³⁰ M. Nakao,⁷ Z. Natkaniec,²⁶ S. Nishida,⁷ O. Nitoh,⁴⁵ S. Noguchi,²² S. Ogawa,³⁹ T. Ohshima,²¹ S. Okuno,¹⁴ H. Ozaki,⁷ P. Pakhlov,¹² G. Pakhlova,¹² H. Palka,²⁶ C. W. Park,³⁷ H. Park,¹⁶ K. S. Park,³⁷ L. S. Peak,³⁸ R. Pestotnik,¹³ L. E. Piilonen,⁴⁶ H. Sahoo,⁶ Y. Sakai,⁷ O. Schneider,¹⁷ R. Seidl,^{8,33} A. Sekiya,²² K. Senyo,²¹ M. Shapkin,¹¹ H. Shibuya,³⁹ J.-G. Shiu,²⁵ J. B. Singh,³² A. Somov,³ S. Stanič,²⁹ M. Starič,¹³ T. Sumiyoshi,⁴⁴ S. Y. Suzuki,⁷ F. Takasaki,⁷ N. Tamura,²⁸ M. Tanaka,⁷ G. N. Taylor,²⁰ Y. Teramoto,³⁰ I. Tikhomirov,¹² K. Trabelsi,⁷ S. Uehara,⁷ T. Uglov,¹² Y. Unno,⁵ S. Uno,⁷ P. Urquijo,²⁰ Y. Usov,¹ G. Varner,⁶ K. Vervink,¹⁷ C. H. Wang,²⁴ M.-Z. Wang,²⁵ P. Wang,⁹ Y. Watanabe,¹⁴ R. Wedd,²⁰ E. Won,¹⁵ B. D. Yabsley,³⁸ H. Yamamoto,⁴¹ Y. Yamashita,²⁷ Z. P. Zhang,³⁵ V. Zhilich,¹ A. Zupanc,¹³ and O. Zyukova¹

(The Belle Collaboration)

¹*Budker Institute of Nuclear Physics, Novosibirsk*

²*Chiba University, Chiba*

³*University of Cincinnati, Cincinnati, Ohio 45221*

⁴*The Graduate University for Advanced Studies, Hayama*

⁵*Hanyang University, Seoul*

⁶*University of Hawaii, Honolulu, Hawaii 96822*

⁷*High Energy Accelerator Research Organization (KEK), Tsukuba*

⁸*University of Illinois at Urbana-Champaign, Urbana, Illinois 61801*

⁹*Institute of High Energy Physics, Chinese Academy of Sciences, Beijing*

¹⁰*Institute of High Energy Physics, Vienna*

¹¹*Institute of High Energy Physics, Protvino*

¹²*Institute for Theoretical and Experimental Physics, Moscow*

¹³*J. Stefan Institute, Ljubljana*

¹⁴*Kanagawa University, Yokohama*

¹⁵*Korea University, Seoul*

¹⁶*Kyungpook National University, Taegu*

¹⁷*École Polytechnique Fédérale de Lausanne (EPFL), Lausanne*

¹⁸*Faculty of Mathematics and Physics, University of Ljubljana, Ljubljana*

¹⁹*University of Maribor, Maribor*

²⁰*University of Melbourne, School of Physics, Victoria 3010*

²¹*Nagoya University, Nagoya*

²²*Nara Women's University, Nara*

²³*National Central University, Chung-li*

²⁴*National United University, Miao Li*

²⁵*Department of Physics, National Taiwan University, Taipei*

²⁶*H. Niewodniczanski Institute of Nuclear Physics, Krakow*

²⁷*Nippon Dental University, Niigata*

²⁸*Niigata University, Niigata*

²⁹*University of Nova Gorica, Nova Gorica*

³⁰*Osaka City University, Osaka*

³¹*Osaka University, Osaka*

³²*Panjab University, Chandigarh*

³³*RIKEN BNL Research Center, Upton, New York 11973*

³⁴*Saga University, Saga*

³⁵*University of Science and Technology of China, Hefei*

³⁶Seoul National University, Seoul

³⁷Sungkyunkwan University, Suwon

³⁸University of Sydney, Sydney, New South Wales

³⁹Toho University, Funabashi

⁴⁰Tohoku Gakuin University, Tagajo

⁴¹Tohoku University, Sendai

⁴²Department of Physics, University of Tokyo, Tokyo

⁴³Tokyo Institute of Technology, Tokyo

⁴⁴Tokyo Metropolitan University, Tokyo

⁴⁵Tokyo University of Agriculture and Technology, Tokyo

⁴⁶Virginia Polytechnic Institute and State University, Blacksburg, Virginia 24061

⁴⁷Yonsei University, Seoul

(Dated: November 3, 2018)

We present a measurement of the branching fraction $B(D_s^+ \rightarrow \mu^+ \nu_\mu)$ using a 548 fb^{-1} data sample collected by the Belle experiment at the KEKB e^+e^- collider. The D_s momentum is determined by reconstruction of the system recoiling against $DK\gamma X$ in events of the type $e^+e^- \rightarrow D_s^* DKX$, $D_s^* \rightarrow D_s \gamma$, where X represents additional pions or photons from fragmentation. The full reconstruction method provides high resolution in the neutrino momentum and thus good background separation, equivalent to that reached by experiments at the tau-charm factories. We obtain the branching fraction $B(D_s^+ \rightarrow \mu^+ \nu_\mu) = (6.44 \pm 0.76(\text{stat}) \pm 0.57(\text{syst})) \cdot 10^{-3}$, implying a D_s decay constant of $f_{D_s} = (275 \pm 16(\text{stat}) \pm 12(\text{syst})) \text{ MeV}$.

PACS numbers: 13.20.-v, 13.20.Fc

One of the important goals of particle physics is the precise measurement and understanding of the Cabibbo-Kobayashi-Maskawa (CKM) matrix elements, fundamental parameters of the Standard Model (SM). To interpret precise experimental results on decays of B mesons in terms of the CKM matrix elements, theoretical calculations of form factors and decay constants (usually based on lattice gauge theory, see e.g. [1]) are needed. Decays of charmed hadrons in turn enable tests of the predictions for analogous quantities in the charm sector. Measurements of charmed meson decay rates with an accuracy that matches the precision of theoretical calculations is thus necessary for checks and further tuning of theoretical methods.

The purely leptonic decay $D_s^+ \rightarrow \ell^+ \nu_\ell$ (the charge-conjugate mode is implied throughout this paper) is theoretically rather clean; in the SM, the decay is mediated by a single virtual W^\pm boson. The decay rate is given by

$$\Gamma(D_s^+ \rightarrow \ell^+ \nu_\ell) = \frac{G_F^2}{8\pi} f_{D_s}^2 m_\ell^2 m_{D_s} \left(1 - \frac{m_\ell^2}{m_{D_s}^2}\right)^2 |V_{cs}|^2, \quad (1)$$

where G_F is the Fermi coupling constant, m_ℓ and m_{D_s} are the masses of the lepton and of the D_s meson, respectively. V_{cs} is the corresponding CKM matrix element, while all effects of the strong interaction are accounted for by the decay constant f_{D_s} . While the decay rate is tiny for electrons due to the strong helicity suppression and since the detection of τ 's involve additional neutrinos, the muon mode is experimentally the cleanest and the most accessible one. Decays with electrons can be used to study the backgrounds.

The analysis described in this paper uses data from the

Belle experiment [2] at the KEKB collider [3] corresponding to 548 fb^{-1} . We study the decay $D_s^+ \rightarrow \mu^+ \nu_\mu$ using the full-reconstruction recoil method first established in the study of semileptonic D mesons [4]. Similar analyses have also been performed by the CLEO-c [5] and BaBar [6] experiments.

The Belle detector is a large-solid-angle magnetic spectrometer that consists of a silicon vertex detector (SVD), a 50-layer central drift chamber (CDC), an array of aerogel threshold Cherenkov counters (ACC), a barrel-like arrangement of time-of-flight scintillation counters (TOF), and an electromagnetic calorimeter comprised of CsI(Tl) crystals (ECL) located inside a superconducting solenoid coil that provides a 1.5 T magnetic field. An iron flux-return located outside of the coil is instrumented to detect K_L^0 mesons and to identify muons (KLM). The detector is described in detail elsewhere [2]. Two inner detector configurations were used. A 2.0 cm beampipe and a 3-layer silicon vertex detector were used for the first sample of 156 fb^{-1} , while a 1.5 cm beampipe, a 4-layer silicon detector and a small-cell inner drift chamber were used to record the remaining 392 fb^{-1} [7].

This analysis uses events of the type $e^+e^- \rightarrow D_s^* D^{\pm,0} K^{\pm,0} X$, where X can be any number of additional pions from fragmentation, and up to one photon [8]. The *tag side* consists of a D and a K meson (in any charge combination) while the *signal side* is a D_s^* meson decaying to $D_s \gamma$. Reconstructing the tag side, and allowing any possible set of particles in X , the signal side is identified by reconstruction of the recoil mass, using the known beam momentum and four-momentum conservation.

Tracks are detected with the CDC and the SVD. They

are required to have at least one associated hit in the SVD and an impact parameter with respect to the interaction point of less than 2 cm in the radial direction and less than 4 cm in the beam direction. Tracks are also required to have momenta in the laboratory frame greater than 100 MeV/c. A likelihood ratio for a given track to be a kaon or pion, $\mathcal{L}(K, \pi)$, is obtained by utilizing specific ionization energy loss measurements in the CDC, light yield measurements from the ACC, and time-of-flight information from the TOF [9]. We require $\mathcal{L}(K, \pi) > 0.5$ for kaon candidates. The momentum of the lepton candidates is required to be larger than 500 MeV/c. For electron identification we use position, cluster energy, shower shape in the ECL, combined with track momentum and dE/dx measurements in the CDC and hits in the ACC. For muon identification, we extrapolate the CDC track to the KLM and compare the measured range and transverse deviation in the KLM with the expected values. Photons are required to have energies in the laboratory frame of at least 50 - 150 MeV, depending on the detecting part of the ECL. Neutral pion candidates are reconstructed using photon pairs with invariant mass within ± 10 MeV/c² of the nominal π^0 mass. Neutral kaon candidates are reconstructed using charged pion pairs with invariant mass within ± 30 MeV/c² of the nominal K^0 mass.

Charged and neutral tag-side D mesons are reconstructed in $D \rightarrow K n \pi$ decays with $n = 1, 2, 3$ (total branching fraction $\approx 25\%$). Mass windows were optimized for each channel separately, and a mass-constrained vertex fit (requiring a confidence level greater than 0.1%) is applied to the D meson to improve the momentum resolution. D_s^* -candidates are not directly reconstructed: we construct the mass of the system recoiling against DKX , using the known beam momentum, and require a value within ± 150 MeV/c² of the nominal D_s^* mass [10]. A recoil mass $M_{\text{rec}}(Y)$ is defined as the magnitude of the four-momentum $p_{\text{beams}} - p_Y$, for an arbitrary set of reconstructed particles Y . p_{beams} is the momentum of the initial e^+e^- system. Since at this point in the reconstruction X can be any set of remaining pions and photons, there is usually a large number of combinatorial possibilities. It is reduced by requiring the presence of a photon that is consistent with the decay $D_s^* \rightarrow D_s \gamma$, where the D_s mass lies within ± 150 MeV/c² of its nominal mass [10]. Further selection criteria are applied on the momenta of particles in the e^+e^- rest frame; for the primary K meson the momentum should be smaller than 2 GeV/c, for the D meson larger than 2 GeV/c and for the D_s meson larger than 3 GeV/c. The energy of the photon from $D_s^* \rightarrow D_s \gamma$ in the lab frame is required to be larger than 150 MeV, irrespective of its polar angle. To further improve the recoil momentum resolution, inverse [11] mass-constrained vertex fits are then performed for the D_s^* and D_s , requiring a confidence level greater than 1%. After implying these selection criteria, the aver-

age number of combinatorial reconstruction possibilities is approximately 2 per event. The sample is further divided into a right- (RS) and wrong-sign (WS) part. If the primary K meson is charged, both it and the D meson are required to have opposite flavor (strangeness or charm respectively) to the D_s^* , to be counted in the right-sign sample; all other combinations are wrong-sign. If the primary K meson is a K_S^0 , the assignment is based on the relative flavor of the D and D_s^* mesons alone. The flavor of the D_s^* is fixed by the total charge of the X , assuming overall charge conservation for the event.

Within this sample of tagged inclusive D_s decays (named D_s -tags in the following), decays of the type $D_s \rightarrow \mu \nu \mu$ are selected by requiring another charged track that is identified as a muon and has the same charge as the D_s candidate. No additional charged particles are allowed in the event. Remaining photons not used in the described reconstruction are allowed only if their total energy is smaller than $1.0/m$ GeV, where m is the number of such particles. After these selections, in almost all cases only one combinatorial reconstruction possibility remains. Figure 1 shows the mass spectra of $M_{\text{rec}}(DKX\gamma)$ (corresponding to the candidate D_s mass) and of $M_{\text{rec}}(DKX\gamma\mu)$ (corresponding to the neutrino candidate mass).

We define n_X as the number of *primary* particles in the event, where primary means that the particle is not a daughter of any particle reconstructed in the event. The minimal value for n_X is three corresponding to a $e^+e^- \rightarrow D_s^* DK$ event without any further particles from fragmentation. The upper limit for n_X is determined by the reconstruction efficiency; Monte Carlo (MC) simulation shows that the number of reconstructed signal events is negligible for $n_X > 10$. As the efficiency very sensitively depends on n_X , it is crucial to use MC simulation that correctly reflects the n_X distribution observed in the data. Unfortunately, the details of fragmentation processes are not very well understood, and standard MC events show notable differences compared to the data. Furthermore, the true (generated) n_X^T value differs from the reconstructed n_X^R , as particles can be lost or wrongly assigned. Thus the measured (reconstructed) n_X^R distribution has to be deconvoluted so that the analysis can be done in bins of n_X^T to avoid bias in the results.

To extract the number of D_s -tags as a function of n_X^T in data, two dimensional simulated distributions in n_X^R (ranging from 3 to 8) and the recoil mass $M_{\text{rec}}(DKX\gamma)$ are fitted to the RS and WS data distributions. The signal shapes for different values of n_X^T (ranging from 3 to 9 [12]) of the signal are modeled with generic MC simulation [13], which has been filtered at the generator level for events of the type $e^+e^- \rightarrow D_s^* DKX$. The weights of these components, $w_i^{D_s^*}$, $i = 3, \dots, 8$, are free parameters in the fit to the data. As a model for the background in the RS sample, the WS data sample is used. The normalization constants between WS and RS (which vary

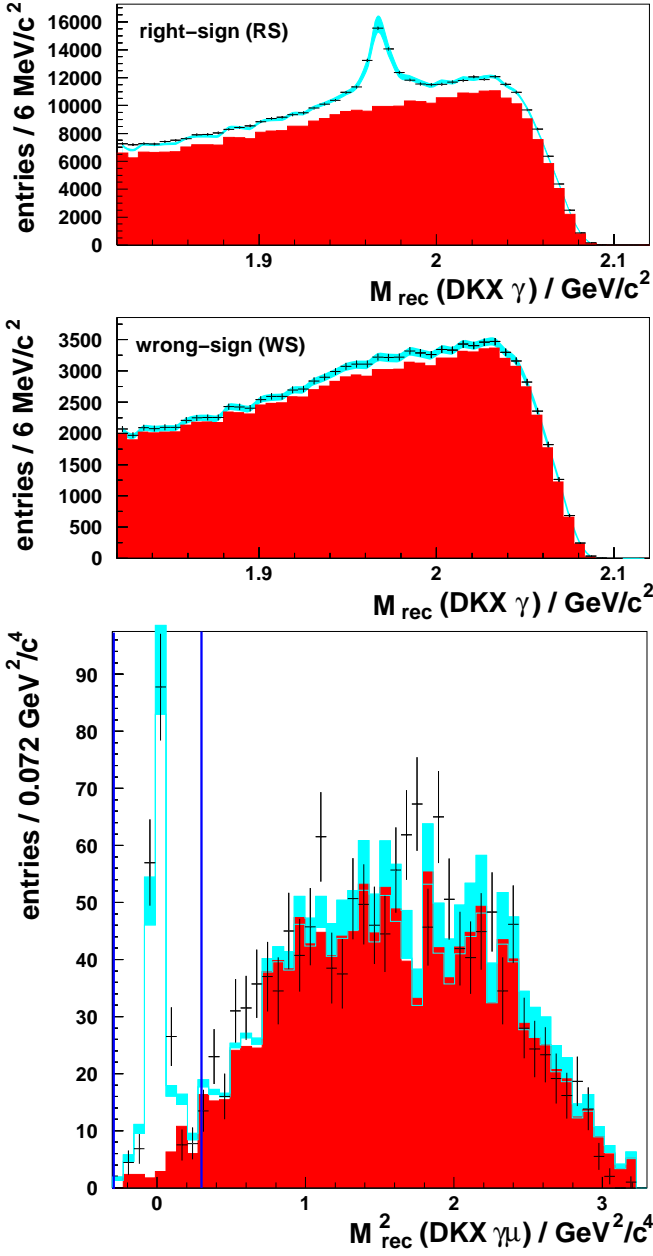


FIG. 1: Top: recoil mass spectrum for D_s -tags (for both RS and WS samples). Bottom: spectrum of missing mass squared for $D_s^+ \rightarrow \mu^+ \nu_\mu$ candidates for the selected data. Error bars represent the statistical errors. The dark-shaded areas show the fitted background, the light-shaded bands show the fit with systematic uncertainties. The vertical lines indicate the signal regions.

with n_X^R) are another six fit parameters. Since the WS sample contains some signal ($\approx 10\%$ of the RS signal), these signal components for different n_X^T values are also included in the fit as independent parameters. As a cross-check, the fit has also been performed using generic MC RS-sample backgrounds, which gives a negligible change in the results. A further cross-check involved the random division of the MC sample into two halves, using

the shapes of the first half to fit the signal in the second. The resulting weights as function of n_X^T fit to a constant of 0.990 ± 0.046 , which agrees well with the expectation of 1. The total number of reconstructed D_s -tags in data is calculated as

$$N_{D_s}^{\text{rec}} = \sum_{i=3}^8 w_i^{D_s} N_{D_s}^{\text{MC},i} , \quad (2)$$

where $N_{D_s}^{\text{MC},i}$ represents the total number of reconstructed filtered MC events that were generated with $n_X^T = i$ (regardless of the reconstructed n_X^R) and $w_i^{D_s}$ the fitted weight of this component.

To fit the number of $D_s \rightarrow \mu\nu_\mu$ events as a function of n_X^T , two-dimensional histograms in n_X^R and the recoil mass $M_{\text{rec}}(DKX\gamma\mu)$ are used. The shape of the signal is modeled with signal MC distribution. As MC studies show, the background under the $\mu\nu_\mu$ signal peak consists primarily of non- D_s decays ($\approx 18\%$ of signal), leptonic τ decays (where the τ decays to a muon and two neutrinos, $\approx 7\%$) and semileptonic D_s decays (where the additional hadrons have low momenta and remain undetected, $\approx 3.6\%$). Hadronic D_s decays (with one hadron misidentified as a muon) are a rather small background component ($\leq 2\%$ of signal). Except for hadronic decays, which are negligible, all backgrounds are common to the $e\nu_e$ mode, which is suppressed by a factor of $\mathcal{O}(10^5)$. Thus, the $e\nu_e$ sample provides a good model of the $\mu\nu_\mu$ background that has to be corrected only for kinematical and efficiency differences. Including this corrected shape in the fit, the total number of fitted $\mu\nu_\mu$ events in data is given by

$$N_{\mu\nu}^{\text{rec}} = \sum_{i=3}^8 w_i^{\mu\nu} N_{\mu\nu}^{\text{MC},i} , \quad (3)$$

where $N_{\mu\nu}^{\text{MC},i}$ represents the total number of reconstructed signal MC events that were generated in the i -th bin of n_X^T (regardless of the reconstructed n_X^R) and $w_i^{\mu\nu}$ is the fitted weight of this component.

The numerical result for $N_{D_s}^{\text{rec}}$ is $32100 \pm 870(\text{stat}) \pm 1210(\text{syst})$, that for $N_{\mu\nu}^{\text{rec}}$ is $169 \pm 16(\text{stat}) \pm 8(\text{syst})$. The statistical errors reflect the finite number of data signal candidates. The systematic errors are due to the limited statistics of WS data and MC signal and background samples. The errors were estimated by varying the bin contents of data and MC distributions and repeating the fits. By this procedure the non-negligible correlations among the fitted weights were taken into account.

As the branching fraction of $D_s \rightarrow \mu\nu_\mu$ used for the generation of MC events is known, the branching fraction in data can be determined using the following formula:

$$\mathcal{B}(D_s \rightarrow \mu\nu_\mu) = \frac{N_{\mu\nu}^{\text{rec}}}{\bar{\epsilon}_{\mu\nu} N_{D_s}^{\text{rec}}} = \frac{N_{\mu\nu}^{\text{rec}}}{N_{\mu\nu}^{\text{MC,rec}}} \mathcal{B}_{\text{MC}}(D_s \rightarrow \mu\nu_\mu) , \quad (4)$$

where $\mathcal{B}_{\text{MC}}(D_s \rightarrow \mu\nu_\mu) = 0.51\%$ and $N_{\mu\nu}^{\text{MC,rec}}$ is the number of reconstructed $\mu\nu_\mu$ events in MC simulation, weighted according to the fit to data, i.e.

$$N_{\mu\nu}^{\text{MC,rec}} = \sum_{i=3}^8 w_i^{D_s} N_{\mu\nu}^{\text{MC},i}. \quad (5)$$

The average efficiency for the reconstruction of $D_s \rightarrow \mu\nu_\mu$ decays, $\bar{\epsilon}_{\mu\nu}$, is not needed explicitly for the computation of the branching fraction [14]. The final result is:

$$\mathcal{B}(D_s \rightarrow \mu\nu_\mu) \cdot 10^3 = 6.44 \pm 0.76(\text{stat}) \pm 0.57(\text{syst}). \quad (6)$$

The quoted statistical error reflects the statistical uncertainty of the fitted weights $w_i^{D_s}$ and $w_i^{\mu\nu}$, including their correlations. The systematic error combines the contributions due to the statistical uncertainties of data and MC background samples (0.29), the statistical uncertainty of the signal MC distribution (0.41), muon tracking and identification efficiency (0.18) and possible differences in relative rates of individual D_s decay modes between MC simulation and data (0.19). Since the branching fraction is determined relative to the number of D_s -tags, the systematic errors in the reconstruction of the tag side cancel. Differences in the neutrino peak resolution between data and simulation have been found to have a negligible effect on the systematic error.

Figure 2 (top) shows the branching fraction determined in bins of n_X^T . The result is stable within errors in n_X^T ; note that the errors shown for the n_X^T bins are correlated. As a cross check, also the branching fraction in a limited range $n_X^T \leq 6$ has been determined as $(6.54 \pm 0.76(\text{stat}) \pm 0.57(\text{syst})) \cdot 10^{-3}$, which agrees well with the result given above. Figure 2 (bottom) shows our result in comparison with the PDG [10] value and recent results from other experiments [5, 6].

In conclusion, we have studied events of the type $e^+e^- \rightarrow D_s^* D^{\pm,0} K^{\pm,0} X, D_s^* \rightarrow D_s \gamma$ with $X = n\pi(\gamma)$ where the D_s is identified in the recoil of the remainder of the event. Normalizing to this sample of D_s -tags, the branching fraction of $D_s \rightarrow \mu\nu_\mu$ was measured to be $(6.44 \pm 0.76(\text{stat}) \pm 0.57(\text{syst})) \cdot 10^{-3}$, which is in good agreement with the current PDG value of $(6.1 \pm 1.9) \cdot 10^{-3}$ [10] and also compatible with recent results from BaBar $(6.74 \pm 1.09) \cdot 10^{-3}$ [6] and CLEO-c $(5.94 \pm 0.73) \cdot 10^{-3}$ [5]. Finally we obtain the decay constant f_{D_s} , using Eqn. (1) (with $|V_{cs}| = 0.9730$ [10])

$$f_{D_s} = (275 \pm 16(\text{stat}) \pm 12(\text{syst})) \text{ MeV}. \quad (7)$$

A simple average of the decay constants following from the cited measurements has an uncertainty of around 10 MeV. Recently an LQCD calculation of significantly improved precision was performed, with the result $f_{D_s} = (241 \pm 3) \text{ MeV}$ [15]. This value is somewhat lower than the experimental average and the comparison with the experimental results may point to some inconsistency between the two. More precise measurements are needed

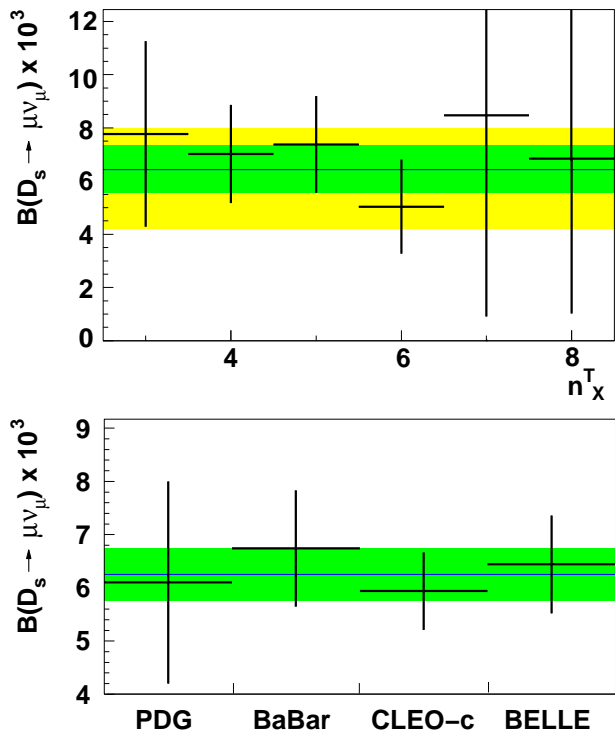


FIG. 2: Top: $\mathcal{B}(D_s \rightarrow \mu\nu_\mu)$ as a function of n_X^T ; the final result is shown as the dark-shaded region. For comparison, the PDG value and its error is shown as the light-shaded region in the background. Bottom: our result compared with PDG [10] and recent BaBar [6] and CLEO-c [5] measurements not yet included in the PDG 2006 compilation; the dark-shaded region shows the weighted average of all measurements.

for a firm comparison and will become possible in the near future at both B and tau-charm factories.

We thank the KEKB group for excellent operation of the accelerator, the KEK cryogenics group for efficient solenoid operations, and the KEK computer group and the NII for valuable computing and Super-SINET network support. We acknowledge support from MEXT and JSPS (Japan); ARC and DEST (Australia); NSFC and KIP of CAS (contract No. 10575109 and IHEP-U-503, China); DST (India); the BK21 program of MOEHRD, and the CHEP SRC and BR (grant No. R01-2005-000-10089-0) programs of KOSEF (Korea); KBN (contract No. 2P03B 01324, Poland); MES and RFAAE (Russia); ARRS(Slovenia); SNSF (Switzerland); NSC and MOE (Taiwan); and DOE (USA).

-
- [1] A. S. Kronfeld (Fermilab Lattice Collaboration), J. Phys. Conf. Ser. **46**, 147 (2006).
 - [2] A. Abashian *et al.* (Belle Collab.), Nucl. Instr. and Meth. **A479**, 117 (2002).
 - [3] S. Kurokawa and E. Kikutani (Belle), Nucl. Instr. and Meth. **A499**, 1 (2003), and other papers in this volume.

- [4] L. Widhalm *et al.* (Belle Collab.), Phys.Rev.Lett. **97**, 061804 (2006).
- [5] M. Artuso *et al.* (CLEO-c Collab.), Phys.Rev.Lett. **99**, 071802 (2007).
- [6] B. Aubert *et al.* (BABAR Collab.), Phys. Rev.Lett. **98**, 141801 (2007).
- [7] Z. Natkaniec *et al.* (Belle SVD2 Group), Nucl. Instr. and Meth. **A560**, 1 (2006).
- [8] It has been found that events with additional kaons or more than one photon have a poor signal/background ratio and have been therefore excluded.
- [9] E. Nakano, Nucl. Instrum. Meth. **A494**, 402 (2002).
- [10] W.-M. Yao *et al.* (Particle Data Group), J. Phys. **G33**, 1 (2006).
- [11] The fit is called inverse since it uses information from the mother and sister particles, rather than information about daughter particles as is usually the case.
- [12] The upper limit of 9 is chosen because the bin $n_X^T = 9$ has some overlap with $n_X^R \leq 8$. The corresponding fitted weight turns out to be negligible and is neglected in the further analysis.
- [13] R. Brun *et al.*, GEANT 3.21, CERN Report DD/EE/84-1, 1984.
- [14] As defined in equation (4), the average efficiency $\bar{\epsilon}_{\mu\nu} = \sum_{i=1}^8 (w_i^{D_s} N_{\mu\nu}^{MC,i}) / \sum_{i=1}^8 (w_i^{D_s} N_{\mu\nu}^{MC,i} / \epsilon_i)$.
- [15] E. Follana *et al.* (HPQCD and UKQCD Collab.), Phys.Rev.Lett. **100**, 062002 (2008).